Hindawi
Advances in Materials Science and Engineering
Volume 2022, Article ID 4297649, 8 pages
https://doi.org/10.1155/2022/4297649

Research Article

Calculation of the Overall Coordination Internal Force of the Grille Beam-Column under the Impact of Debris Flow

Yongsheng Wang,[1,2] **Hao Zhu**,[1,2] **and Bing Wang**[1,2]

[1]*School of Civil Engineering, Lanzhou University of Technology, Lanzhou 730050, China*
[2]*Western Center for Disaster Mitigation in Civil Engineering of Ministry of Education, Lanzhou University of Technology, Lanzhou 730050, China*

Correspondence should be addressed to Yongsheng Wang; wys5918@lut.edu.cn

Received 9 March 2022; Accepted 5 May 2022; Published 15 June 2022

Academic Editor: Qian Chen

Copyright © 2022 Yongsheng Wang et al. This is an open access article distributed under the Creative Commons Attribution License, which permits unrestricted use, distribution, and reproduction in any medium, provided the original work is properly cited.

At present, the research on the new ground anchor counterfort grille dam is not perfect. In order to analyze and design the new grille dam accurately and reasonably, it is necessary to carry out theoretical research on the internal force calculation of the overall coordination of the grille beam-column under the impact of debris flow. Under the condition of full reservoir of debris flow, the grille beam-column meets the working principle of elastic foundation beam; therefore, the equation of the overall cooperative work of the grille beam-column is derived based upon Winkler's theory of elastic foundation beam. Finally, combined with the engineering example, this calculation method is used for analysis; the results show that the bending moment of the grille beam-column increases compared with that regardless of considering the overall coordination, and the increased value of the bending moment at the bottom of the grille column and the middle of the grille beam is the largest. Therefore, from the perspective of safety, the overall coordination cannot be ignored when designing a blocking dam.

1. Introduction

China is a region with frequent debris flow outbreaks, most of which are in the central and western regions. Every year, the loss of life and property caused by debris flow is extremely serious [1]. As a main protective measure, control structure is always the research focus. With the continuous progress of research, various control structures with different forms and functions have emerged. Liu et al. [2] put forward a new suspended debris flow grille-dam structure; the advantages and disadvantages of this type of dam are obtained by expounding its application in debris flow control engineering of rare debris flow and high sediment flood of debris flow. Su et al. [3] proposed a flexible stone cage intercepting dam structure; numerical simulation is performed using the software ANSYS LS-DYNA and focuses on the dynamic response of the structure to the impact of the debris flows, and the stress of the dam varies with height under the static calculation condition is obtained. Wang and Zhang [4] proposed a new debris flow grille-dam with friction damper and used ABAQUS finite element software to simulate the impact of debris flow block stone on this new dam. Li et al. [5] proposed the Gabion-pile-slab wall debris flow composite retaining structure; through the experiment, the impact force of each layer of pressure box over time is obtained, which shows that the structure has good stability and anti-overturning ability, and the blocking effect is obvious. Ran et al. [6] proposed a concrete filled steel tubular grille-dam, the dynamic response of the structure was studied by solid impact test, and the test process was numerically simulated. Li et al. [7] proposed a new steel-concrete composite retaining dam and compared the dynamic response of the traditional gravity dam and the improved new retaining dam by using experimental research and numerical simulation. Xie et al. [8] proposed a herringbone water-sediment separation structure, simplified the calculation model of the rib beam, and established the strength calculation formula of the rib beam. Chen et al. [9] proposed the closure dam according to the geographical conditions of Sichuan Province, used the latest method to

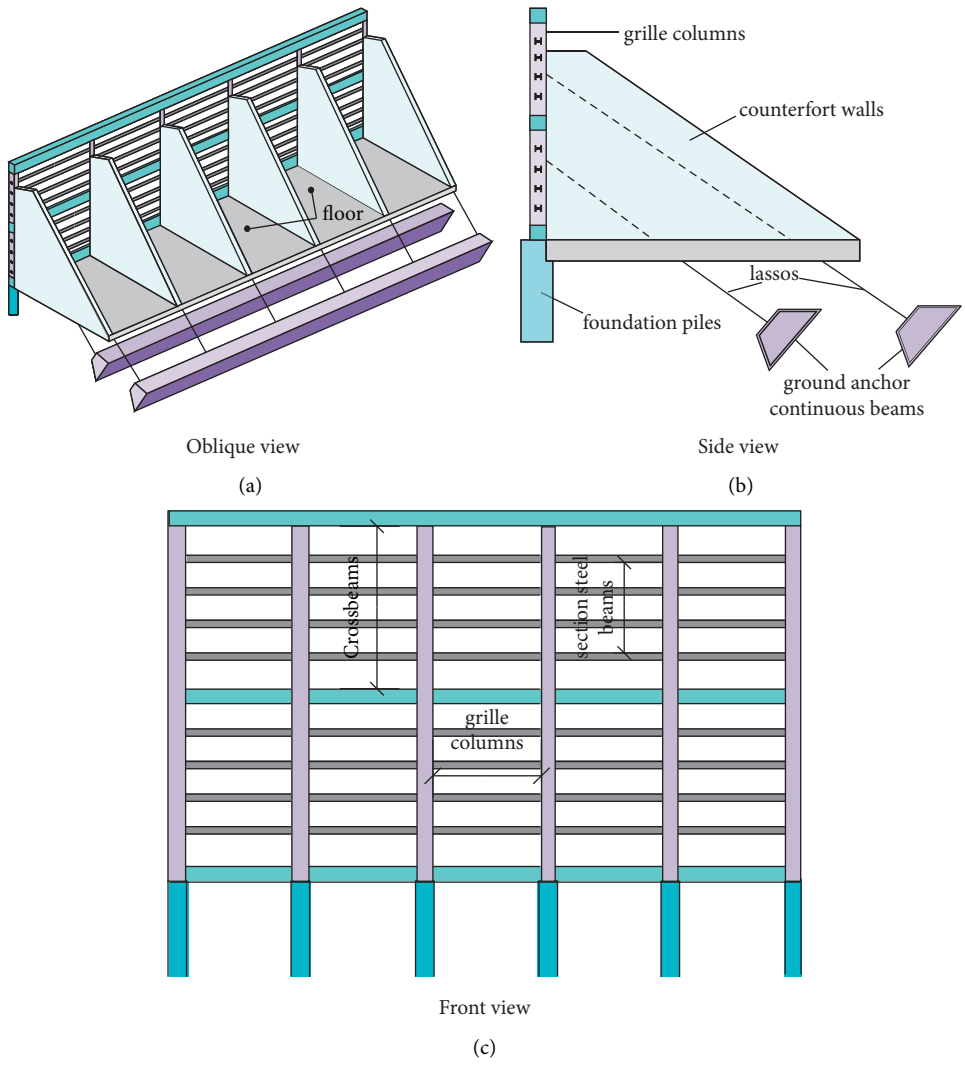

Figure 1: Schematic diagram of new grille-dam. (a) Oblique view, (b) side view, and (c) front view.

evaluate the debris flow, and proposed the control measures of the closure dam according to the results. Zhang et al. [10] proposed an archless debris flow dam based on the mechanical characteristics of the arch and solved the internal force of the arch dam by using the legislative principle in structural mechanics.

In summary, the researchers put forward many new prevention measures for debris flow prevention project. However, the research on the new of retaining dam focuses on numerical simulation and experimental research, which needs a lot of time to establish and analyze the model. Therefore, in this study, Wang et al. [11] proposed a new ground anchor counterfort grille-dam structure (hereinafter called as the new grille-dam). In order to calculate the maximum internal force of grille beam-column more practical, under the condition of full reservoir flow, the debris flow impact force is simplified by calculation as concentrated load reverse action on the grille beam-column node, the grille beam-column is regarded as a whole, the elastic frame model of the whole grille beam-column is established by using the elastic foundation beam model, and then, through the displacement coupling of the connection node, the equation of the overall cooperative work of the grille beam-column is derived, and the internal force is calculated, which lays the foundation for the further analysis of the structural performance of the new grille-dam.

2. Stress Analysis of New Grille-dam

2.1. A Brief Introduction of New Grille-dam. The new grille-dam is mainly composed of grille (composed of grille columns, beams, and waste section steel beams), foundation piles, counterfort walls, lassos, anchor pier, floor, and floor beams, as shown in Figure 1. The grille structure of reinforced concrete grille beam and grille column large frame embedded steel beam is adopted to achieve the goal of debris flow interception and drainage. The ground anchor lassos can ensure the overall stability of the new grille-dam [11].

2.2. Load Calculation of Debris Flow. According to [12], the calculation formula of debris flow impact force is

$$F = \alpha\rho v^2, \tag{1}$$

where $\rho = 1.7g/\text{cm}^3$ is the density of debris flow, $\alpha = 1.17$ is dynamic correction factor, and v is debris flow velocity.

In this study, the vertical variation of debris flow impact force is simplified as triangular linear distribution [13].

2.3. Simplification of the Calculation Model. The load acting on the plane normal line of the axis of the grille beam-column belongs to the calculation category of the spatial structure. The grille beam-column not only has bending moment but also has torque. However, in the actual grille beam-column system, the torsional stiffness of the grille beam-column is smaller than the flexural stiffness, which has little effect on the overall structure and can be ignored. Therefore, the main work of this study is to calculate the bending moment of the grille beam column under the overall coordination.

The vertical distribution of debris flow impact force shows the maximum at the bottom and gradually decays to the fluid surface [12]. In order to consider the overall safety, the grille column and the counterfort walls are cast-in-situ as a whole. The counterfort walls section is designed to be the largest at the bottom and the smallest at the top, T-section with a linear change in the middle, as shown in Figure 2. In order to simplify the calculation and convenient engineering application, the stiffness of each section of the grille column is equivalently calculated according to the size of midspan T-sections, as shown in Figure 3. The grille beam is simplified by equal stiffness multispan continuous beam.

Cross-sectional areas are

$$\begin{aligned} A_c &= a_c b_c, \\ A_{fi} &= a_{fi} b_{fi}. \end{aligned} \tag{2}$$

The distance, respectively, from the centroid of each section to the edge $c\ d$ is

$$\begin{aligned} y_1 &= \frac{b_c}{2}, \\ y_2 &= \frac{b_{fi}}{2} + b_c. \end{aligned} \tag{3}$$

The distance from the centroid of any T-section to the edge $c\ d$ can be expressed as

$$y_c = \frac{A_c y_1 + A_{fi} y_2}{A_c + A_{fi}}. \tag{4}$$

Substituting (2) and (3) into (4), we can obtain

$$y_c = \frac{a_c b_c^2 + a_{fi} b_{fi}\left(b_{fi} + 2b_c\right)}{2\left(a_c b_c + a_{fi} b_{fi}\right)}. \tag{5}$$

The moment of inertia of the T-section of the wall can be expressed as

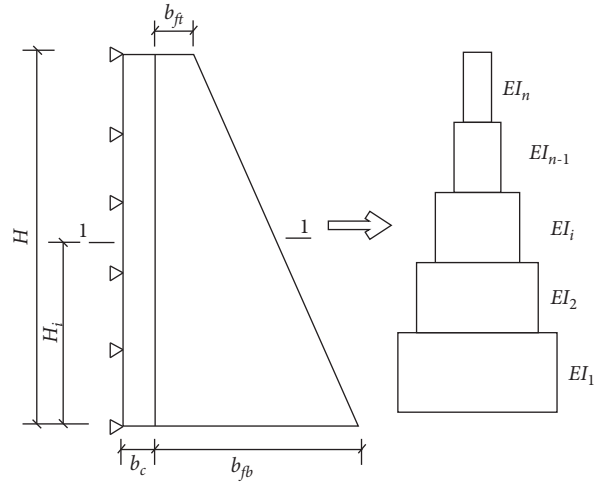

Figure 2: Diagram of equivalent stiffness of grille column and counterfort walls.

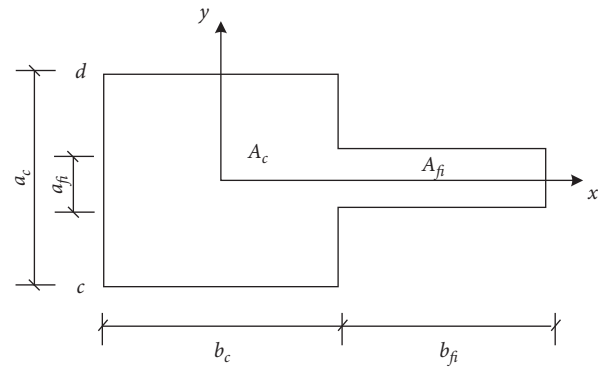

Figure 3: 1-1 sectional view.

$$\begin{aligned} I_{ic} &= \frac{a_c b_c^3}{12} + A_c\left(y_c - y_1\right)^2 \\ &= \frac{a_c b_c^3}{12} + a_c b_c\left[\frac{a_c b_c^2 + a_{fi} b_{fi}\left(b_{fi} + 2b_c\right)}{2\left(a_c b_c + a_{fi} b_{fi}\right)} - \frac{b_c}{2}\right]^2, \\ I_{if} &= \frac{a_{fi} b_{fi}^3}{12} + a_{fi} b_{fi}\left[\frac{a_c b_c^2 + a_{fi} b_{fi}\left(b_{fi} + 2b_c\right)}{2\left(a_c b_c + a_{fi} b_{fi}\right)} - \left(\frac{b_{fi}}{2} + b_c\right)\right]^2, \\ I_i &= I_{ic} + I_{if} \\ &= \frac{a_c b_c^3}{12} + a_c b_c\left[\frac{a_c b_c^2 + a_{fi} b_{fi}\left(b_{fi} + 2b_c\right)}{2\left(a_c b_c + a_{fi} b_{fi}\right)} - \frac{b_c}{2}\right]^2 \\ &\quad + \frac{a_{fi} b_{fi}^3}{12} + a_{fi} b_{fi}\left[\frac{a_c b_c^2 + a_{fi} b_{fi}\left(b_{fi} + 2b_c\right)}{2\left(a_c b_c + a_{fi} b_{fi}\right)} - \left(\frac{b_{fi}}{2} + b_c\right)\right]^2 \\ &= \frac{a_c b_c^3}{12} + a_c b_c\left[\frac{a_c b_c^2 + a_{fi} b_{fi}\left(b_{fi} + 2b_c\right)}{2\left(a_c b_c + a_{fi} b_{fi}\right)} - \frac{b_c}{2}\right]^2, \end{aligned} \tag{6}$$

where A_c, A_{fi}, a_c, b_c, a_{fi}, and b_{fi} represent the cross-sectional area and size of any section of the grille column and the counterfort walls, $y_1 y_2$ is the distance from the centroid

of any section of the grille columns and the counterfort walls to the c d side of the grille column, and y_c is the distance from centroid to edge c d of any T-section.

3. Internal Force Calculation of Grille Beam-Column

At present, there are many studies using Winkel elastic foundation beams to calculate the internal forces of structures at home and abroad. Mudhaffar et al. [14] used the high-order integral shear deformation theory to study the behavior of ceramic-metal plates in viscoelastic foundations under the action of damp heat and thermal loads, the bending equation was investigated, and the effect of temperature and water concentration on the metal plate was investigated. Merazka et al. [15] studied the damp-heat-thermal bending response of a simply supported FG slab on a Winkler–Pasternak elastic foundation under the condition of considering the transverse shear strain and not applying any shear correction factor. Based on the above concepts, in the case of full reservoir flow, debris flow impacts the new grille-dam instantly and debris flow deposits produce compression deformation. It is assumed that the compression deformation of deposits is generated by the reaction of the impact force of debris flow on the grille beam-column joints. Combined with Winkler's theory of elastic foundation beam, considering the constraint of side span grille column, the grille beam is regarded as a short beam with fixed ends, as shown in Figure 4; the grille column is regarded as a semi-infinite beam with fixed end for calculation, as shown in Figure 5.

On the basis of Winkler's assumption, the flexible characteristic values of grille beams and columns are as follows [16]:

$$\lambda_x = \sqrt[4]{\frac{k_0 b_x}{4EI_x}}, \qquad \lambda_y = \sqrt[4]{\frac{k_0 b_y}{4EI_{y(i-1)}}}, \tag{7}$$

where λ_x and λ_y is the rigid and flexible characteristic value of the grille beam-column, k_0 is the foundation coefficient, also called the foundation resistance coefficient, b_x and b_y is the single span of grille beam-column in the x and y directions, E is the elastic modulus of the grille beam-column, and I_x and $I_{y(i-1)}$ is the section moment of inertia of the grille beam-column.

Assuming that the grille beam is parallel to the x-axis direction and the grille column is parallel to the y-axis direction, the bottom of any grille column is taken as the origin of the coordinate axis, and the concentrated force at the intersection of the ith grille beam and the jth grille column is set to P_{ij}, as shown in Figure 6. When a grille beam is subjected to a force, Wenkel assumes that the deformation at any position is as follows [17]:

$$z_{ij}(x) = \frac{P_{xij}\lambda_x}{2k_0 b_x} e^{-\lambda_x X_x} (\cos \lambda_x X_x + \sin \lambda_x X_x), \tag{8}$$

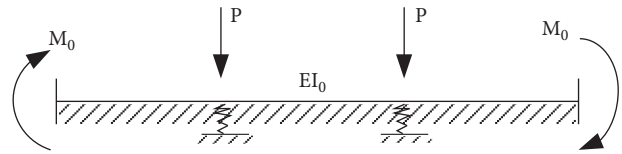

Figure 4: Simplified model of grille beam.

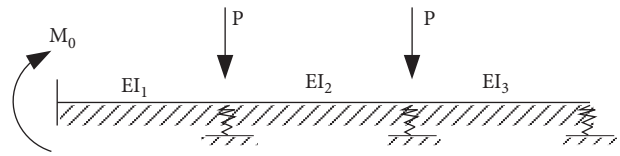

Figure 5: Simplified model of grille column.

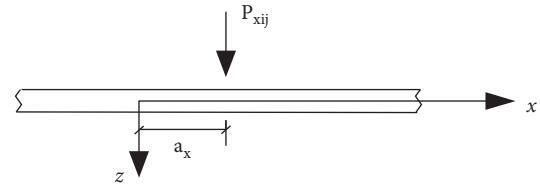

Figure 6: Elastic foundation beam model of grille beam.

where P_{xij} is the force of the debris flow impact force P_{ij} distributed on the grille beam at the intersection of the ith grille beam and the jth grille column, X_x is the distance between the concentrated force P_{xij} on the grille beam and any calculated section position x, and a_x is the distance between the concentrated force P_{xij} on the grille beam and the end point of the grille beam, that is, the origin of the grille beam.

The grille beam and grille column are subjected to multiple concentrated forces at the same time; the deformation of the ith grille beam generated by the superposition method under the action of n concentrated forces is as follows [17]:

$$z'_{ij}(x) = \frac{\lambda_x}{2k_0 b_x} \sum_{j=1}^{n} P_{xij} e^{-\lambda_x X_x} (\cos \lambda_x X_x + \sin \lambda_x X_x). \tag{9}$$

Order

$$\eta_{xij} = \frac{\lambda_x}{2k_0 b_x} e^{-\lambda_x X_x} (\cos \lambda_x X_x + \sin \lambda_x X_x). \tag{10}$$

than

$$\sigma_{xij} = P_{xij}\eta_{xij}, \tag{11}$$

where η_{xij} is the deformation coefficient of the jth node position of the ith grille beam and σ_{xij} is the deformation of the jth node position of the ith grille beam under the action of P_{xij}.

The deformation of all the nodes of the grille beam can be expressed as a matrix:

$$\begin{pmatrix} P_{x11} & \cdots & P_{x1m} \\ \vdots & \ddots & \vdots \\ P_{xn1} & \cdots & p_{xnm} \end{pmatrix} \times \begin{pmatrix} \eta_{x11} & \cdots & \eta_{xn1} \\ \vdots & \ddots & \vdots \\ \eta_{x1m} & \cdots & \eta_{xnm} \end{pmatrix} = \begin{pmatrix} \sigma_{x11} & \cdots & \sigma_{x1m} \\ \vdots & \ddots & \vdots \\ \sigma_{xn1} & \cdots & \sigma_{xnm} \end{pmatrix}. \tag{12}$$

Likewise, as shown in Figure 7, when a grille column is subjected to a force, Winkle assumes that the deformation at any position is as follows:

$$\begin{aligned} z_{ij}(y) = {} & \frac{P_{yij}\lambda_y}{2k_0 b_y} e^{-\lambda_y X_y}\left(\cos\lambda_y X_y + \sin\lambda_y X_y\right) \\ & + \frac{P_{yij}\lambda_y}{k_0 b_y} e^{-\lambda_y a_y} e^{-\lambda_y y}\cos\lambda_y a_y \cos\lambda_y y \\ & - \frac{P_{yij}\lambda_y}{2k_0 b_y} e^{-\lambda_y y} e^{-\lambda_y a_y}\left(\cos\lambda_y y - \sin\lambda_y y\right) \\ & \left(\cos\lambda_y a_y - \sin\lambda_y a_y\right), \end{aligned} \tag{13}$$

where P_{yij} is the force of the debris flow impact force P_{ij} distributed on the grille column at the intersection of the ith grille beam and the jth grille column, X_y is the distance between the concentrated force P_{yij} on the grille column and any calculated section position y, and a_y is the distance between the concentrated force P_{yij} on the grille column and the end point of the grille column, that is, the origin of the grille column.

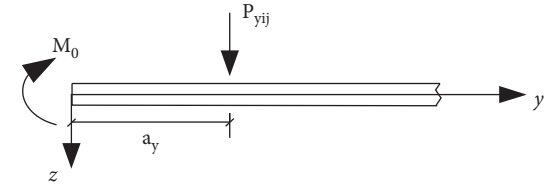

Figure 7: Elastic foundation beam model of grille column.

The deformation of the ith grille column by the superposition method under m concentrated forces is as follows:

$$z'_{ij}(y) = \sum_{i=1}^{m} P_{yij}\left(\begin{array}{l} \dfrac{\lambda_y}{2k_0 b_y} e^{-\lambda_y X_y}\left(\cos\lambda_y X_y + \sin\lambda_y X_y\right) + \dfrac{\lambda_y}{k_0 b_y} e^{-\lambda_y a_y} e^{-\lambda_y y}\cos\lambda_y a_y \cos\lambda_y y \\ \\ \quad - \dfrac{\lambda_y}{2k_0 b_y} e^{-\lambda_y y} e^{-\lambda_y a_y}\left(\cos\lambda_y y - \sin\lambda_y y\right)\left(\cos\lambda_y a_y - \sin\lambda_y a_y\right) \end{array}\right). \tag{14}$$

Order

$$\begin{aligned} \eta_{yji} = {} & \frac{\lambda_y}{2k_0 b_y} e^{-\lambda_y X_y}\left(\cos\lambda_y X_y + \sin\lambda_y X_y\right) \\ & + \frac{\lambda_y}{k_0 b_y} e^{-\lambda_y a_y} e^{-\lambda_y y}\cos\lambda_y a_y \cos\lambda_y y \\ & - \frac{\lambda_y}{2k_0 b_y} e^{-\lambda_y y} e^{-\lambda_y a_y}\left(\cos\lambda_y y - \sin\lambda_y y\right) \\ & \left(\cos\lambda_y a_y - \sin\lambda_y a_y\right). \end{aligned} \tag{15}$$

than

$$\sigma_{yji} = P_{yij}\eta_{yji}, \tag{16}$$

where η_{yji} is the deformation coefficient of the ith node position of the jth grille column and σ_{yji} is the deformation of the ith node position of the jth grille column under the action of P_{yji}.

The deformation of all the nodes of the grille column can be expressed as a matrix:

$$\begin{pmatrix} P_{y11} & \cdots & P_{y1n} \\ \vdots & \ddots & \vdots \\ P_{ym1} & \cdots & p_{ymn} \end{pmatrix} \times \begin{pmatrix} \eta_{y11} & \cdots & \eta_{ym1} \\ \vdots & \ddots & \vdots \\ \eta_{y1n} & \cdots & \eta_{ymn} \end{pmatrix} = \begin{pmatrix} \sigma_{y11} & \cdots & \sigma_{y1m} \\ \vdots & \ddots & \vdots \\ \sigma_{yn1} & \cdots & \sigma_{ynm} \end{pmatrix}. \tag{17}$$

According to the coordination conditions at the grille beam-column joints,

$$\begin{cases} P_{ij} = P_{xij} + P_{yij} \\ \sigma_{xij} = \sigma_{yji}, \end{cases} \tag{18}$$

Comparing the displacement matrix of the grille column and the grille beam node, it is found that the two are transpose matrices, namely, $\sigma_{xij} = \sigma^T_{yji}$.

Thus, (17) can be converted to the following:

$$\begin{pmatrix} \eta_{y11} & \cdots & \eta_{y1n} \\ \vdots & \ddots & \vdots \\ \eta_{ym1} & \cdots & \eta_{ymn} \end{pmatrix} \times \begin{pmatrix} P_{y11} & \cdots & P_{ym1} \\ \vdots & \ddots & \vdots \\ P_{y1n} & \cdots & p_{ymn} \end{pmatrix} = \begin{pmatrix} \sigma_{y11} & \cdots & \sigma_{ym1} \\ \vdots & \ddots & \vdots \\ \sigma_{y1n} & \cdots & \sigma_{ymn} \end{pmatrix}. \tag{19}$$

Combining (12) and (19), P_{xij} and P_{yji} can be obtained by MATLAB software. Finally, P_{xij} and P_{yji} are substituted into (9) and (14) to calculate their deformation, and then, the bending moment equation of the grille beam-column at any cross-section position is obtained by quadratic derivation of (9) and (14).

4. Calculation and Analysis of Engineering Example

4.1. Project Profile. The main design parameters of a new grille-dam are as follows. Concrete grade adopts *C*30, stressed bars for the grille beam-column adopt *HRB*335, stirrups adopt *HPB*300, seven strands of steel strand adopt 3φs15.2, the standard value of single ultimate strength is 1860 N/mm^2, and section area is 140 mm^2; section of grille column is 500 mm × 200 mm, the spacing is 3000 mm; the counterfort wall is the bottom section 600 mm × 200 mm,

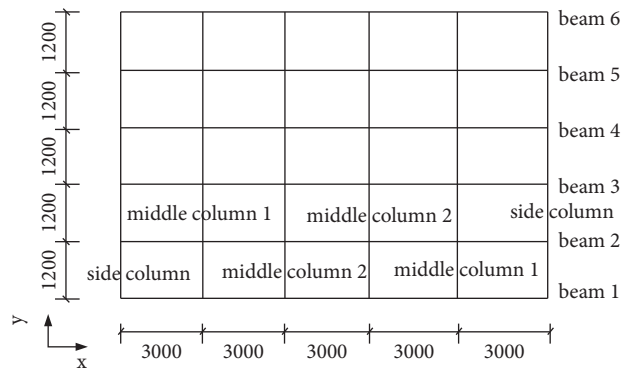

Figure 8: The vertical profile of grille-dam.

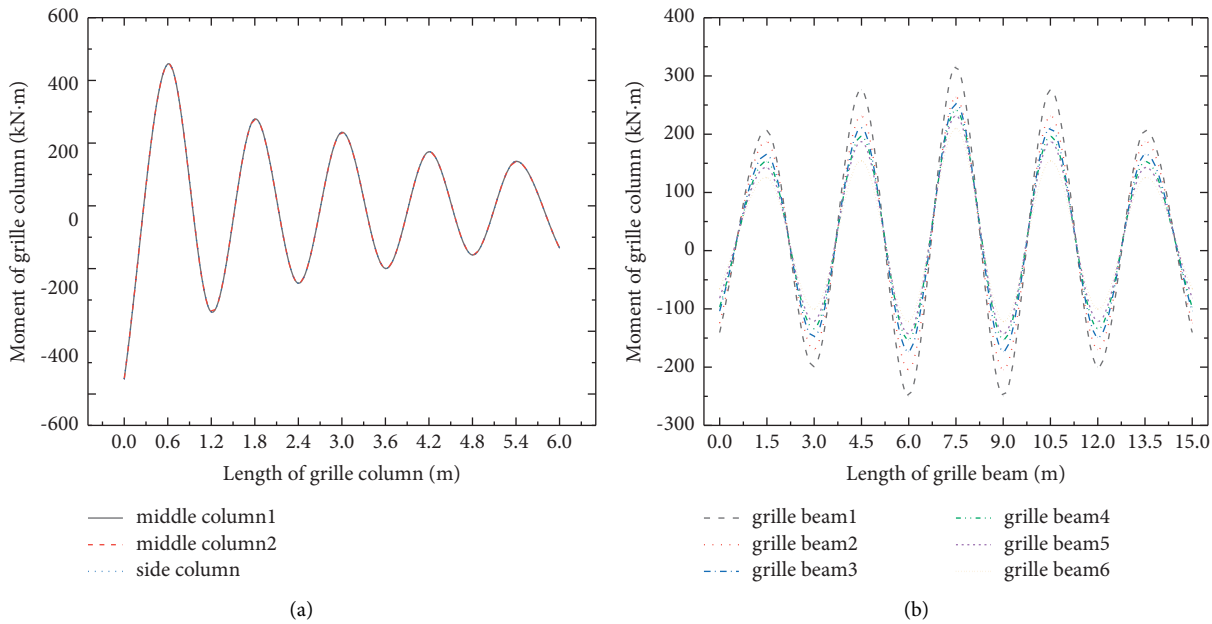

Figure 9: Consider the overall coordination. (a) Bending moment diagram of grille column. (b) Bending moment diagram of grille beam.

the upper section is 300 mm × 200 mm, and the middle section changes linearly; section of grille beam is 400 mm × 200 mm and the spacing is 1200 mm. In the case of full reservoir flow, the maximum velocity is 5 m/s, and the grille beam-column facade is shown in Figure 8.

4.2. Impact of Overall Collaboration on Internal Force Calculation. In order to analyze the influence of the overall coordination on the internal force of the grille beam-column, in the calculation process, the formula considering the overall coordination is first calculated; then, according to [18] regardless the overall coordination, the calculation results are shown in Figures 9 and 10. Because of the symmetry of the grille column, the bending moment only represents the side column, the middle column 1, and the middle column 2. In the figure, the bending moment is positive in the direction of debris flow inflow. The following conclusions can be obtained from Figures 9 and 10.

(1) The bending moment near the inner support of the end span of the grille beam is relatively large. Compared with not considering the overall coordination, the bending moment value of the grille beam increases, the maximum increase is 112.1 kNm, the bending moment value of the grille beam 1 is relatively large, and the maximum value is 546.3 kNm at the midspan position. The cross sections with zero moment are almost on the same vertical line, which indicates that the calculation of grille beams as continuous multispan beams is reasonable, and beam 1 is used as the benchmark in the design of grille beams. Since the velocity of debris flow in the lateral direction is large in the middle and small nonlinear changes on both sides [19], the grille beam 1 with the largest increase in the span direction has an increase of 58.1%, 66.6%, 99.6%, 99.6%, and 66.6%, respectively. The maximum increase position is the midspan, so the design method of variable cross section can be considered when designing grille beams

(2) Under the impact of debris flow, the bending moment at the bottom of the grille column is the largest,

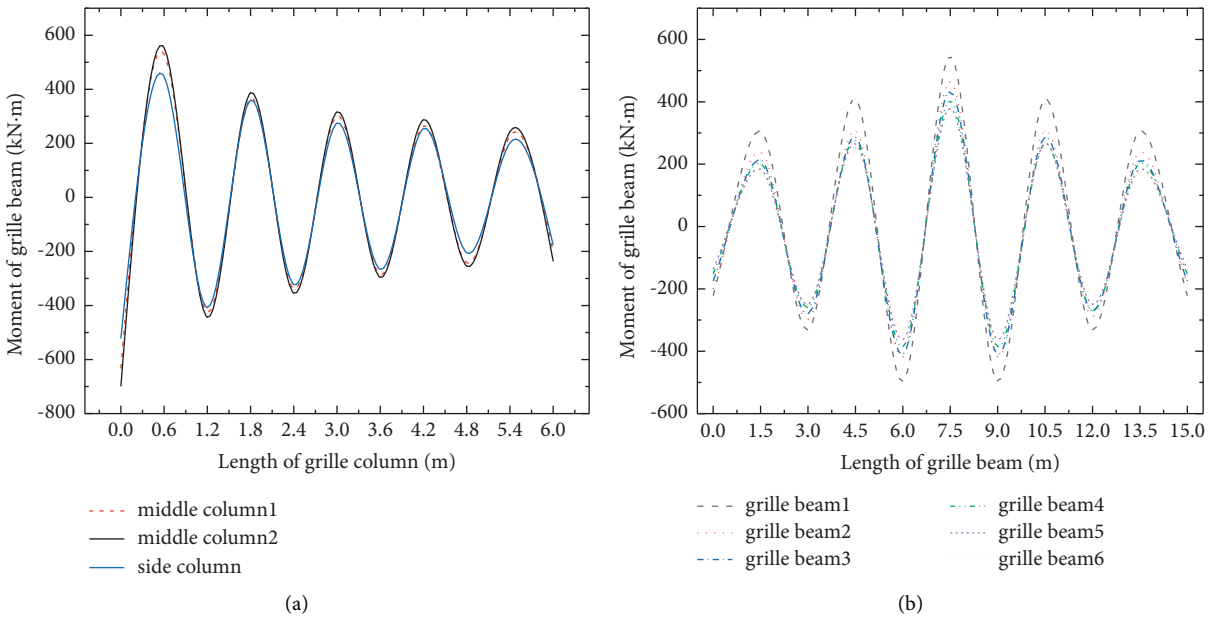

Figure 10: Not considering overall coordination. (a) Bending moment diagram of grille column. (b) Bending moment diagram of grille beam.

which is 698.5 kNm, the bending moment at the upper part is smaller, which is 176.5 kNm, the middle bending moment gradually decreases along the height direction of the grille column, and the decreasing range is 32.5%, 20.5%, 15.4%, 15.3%, and 15.0%, and the decreasing range gradually decreases, because with the increase of height, the stiffness of the grille column gradually decreases. It is small, so the distributed bending moment is reduced, and the impact force of the debris flow is the largest at the bottom and then gradually decays to the fluid surface. The bending moment of the side column is smaller than that of the central column, and after considering the coordination effect, the bending moment values of the central column 1 and 2 both increase, and the bending moment value of the side column shows a decreasing trend due to the constraint effect of the grille beam. It shows that the bearing capacity of the central column should be mainly strengthened in the design of the grille-dam structure.

(3) When do not consider overall coordination, the bending moments of the side column and the center column of the grille-dam are exactly the same. Compared with the results considering the overall coordination, the grille column design without considering the overall coordination is likely to have bottom bending under the impact of debris flow. Shear failure: considering the overall coordination effect, since the stiffness of the grille column is much larger than that of the grille beam, the increase of the bending moment of the grille column is greater than that of the grille beam; when the model is simplified, the end is simplified as a fixed support, so there will be inflection points in the grille beams and columns at equal intervals in the X and Y directions.

5. Conclusions

(1) In this study, the elastic foundation beam theory is used to establish the internal force equation of grille beams and grille columns, and the calculation equation of the overall coordinated internal force of the grille dam is established through equal displacements at the nodes of grille beams and columns, and the obtained results better reflect the grille beams and variation of the internal force of the column.

(2) Engineering analysis and calculation show that, since the stiffness of the grille columns is greater than that of the grille beams, considering the overall coordination effect of the grille columns, the distributed bending moment value is larger, and the increase is more obvious. The increase of the bending moment in the bottom of the grille column and the middle of the grille beam is the largest; the increase in the bending moment of the central column is larger than that of the side column. From the perspective of durability and safety, the overall coordination must be considered when designing new grille dam.

Data Availability

Due to privacy reasons, the data of this paper are temporarily not open to the public.

Conflicts of Interest

The authors declare that they have no conflicts of interest or personal relationships that could have appeared to influence the work reported in this paper.

Authors' Contributions

Yongsheng Wang conceptualized the study, developed methodology, collected resources, administrated the project, carried out funding acquisition, and supervised the study. Hao Zhu conceptualized the study, developed the methodology, curated the data, validated the study, and wrote the original draft. Bing Wang carried out proof reading.

Acknowledgments

This work was financially supported by National Natural Science Foundation of China (Grant no.51768039), Industrial Support Program of Higher Education of Gansu Province (2020C-40), and Hongliu Support Funds for Excellent Youth Talents of Lanzhou University of Technology (Grant nos. 04-062002) and are also highly appreciated.

References

[1] H. L. Pan, Q. G. Ou, and J. F. Liu, "A study on debris-flow gully erosion," *Journal of Catastrophology*, vol. 24, no. 1, pp. 39–43, 2009.

[2] J. B. Liu and L. F. Hou, "The study and application of new jettied crib dam," *Chinese Journal of Geological Hazard and Control*, vol. 25, no. 3, pp. 26–31+37, 2014.

[3] Y. Wang, H. Zhu, and B. Wang, "New technology and numerical simulation of stone cage arch flexible intercepting dam," *Chinese Journal of Geotechnical Engineering*, vol. 37, no. 2, pp. 269–275, 2015.

[4] X. L. Wang and Q. Q. Zhang, "Dynamic responses of a novel debris flow blocking dam with friction damper," *Bulletin of Soil and Water Conservation*, vol. 36, no. 4, pp. 32–35, 2016.

[5] C. H. Li, H. G. Wu, and X. Y. Chen, "Gabion-sheet pile wall structure of debris flow model test," *Chinese Journal of Geological Hazard and Control*, vol. 28, no. 4, pp. 71–76, 2017.

[6] Y. H. Ran, X. L. Wang, and K. Zhou, "Experimental study and parameter analysis on the shock resistance of concrete filled steel tubular crib dam," *Journal of Harbin Institute of Technology*, vol. 50, no. 12, pp. 45–52, 2018.

[7] J. J. Li, X. L. Wang, and Y. H. Ran, "Experimental study dynamic response of a new dam to the impact of block stones in debris flow," *Journal of Harbin Engineering University*, vol. 39, no. 5, pp. 889–896, 2018.

[8] T. Xie, X. P. Xie, F. Q. Wei, and H. Yang, "Structural calculation of herringbone water-sediment separation structure for debris flow defens," *Journal of Sichuan University (Engineering Science Edition)*, vol. 48, no. 2, pp. 48–56, 2016.

[9] J. H. Chen, H. G. Wu, H. H. Zhou, and H. L. Zhang, "Risk assessment and control measure of debris flow in Chunyashu gully of seismic disastrous area of Sichuan province," *Advanced Materials Research*, vol. 446-449, pp. 2988–2991, 2012.

[10] Y. Zhang, Q. Wang, and M. Yin, "Research on non-highed arch dam against debris flow," *Journal of Natural Disasters*, vol. 15, pp. 20–24, 2006.

[11] Y. S. Wang, Y. J. Zhang, Y. P. Zhu, and C. Yan, "Calculation of foundation scour for new debris flow grille-dam with ground anchor and counterfort," *Chinese Journal of Geotechnical Engineering*, vol. 40, no. S1, pp. 272–277, 2018.

[12] D. C. Liu, Y. You, J. Du, J. Liu, J. Guan, and Y. Liu, "Spatio-temporal distribution of the impact force of debris flow," *Advanced Engineering Sciences*, vol. 51, no. 3, pp. 17–25, 2019.

[13] K. C. Wang, X. Zheng, and Y. R. Xia, "Research on damage mechanism of mountain flood disasters to highway bridges in southwest," *Technology of Highway and Transport*, vol. 12, no. 6, pp. 88–93, 2010.

[14] I. M. Mudhaffar, A. Tounsi, A. Chikh, M. A. A. Osta, M. M. A. Zahrani, and S. U. A. Dulaijan, "Hygro-thermo-mechanical bending behavior of advanced functionally graded ceramic metal plate resting on a viscoelastic foundation," *Structures*, vol. 33, pp. 2177–2189, 2021.

[15] B. Merazka, A. Bouhadra, A. Menasria et al., "Hygro-thermo-mechanical bending response of FG plates resting on elastic foundations," *Steel and Composite Structures*, vol. 39, no. 5, pp. 631–643, 2021.

[16] Y. Q. Long, *Calculation of Elastic Foundation Beam*, Beijing People's Education Press, Beijing, China, 1981.

[17] L. Mei, T. M. Zhang, and P. M. Jiang, "Study on load distribution coefficient of lattice beam node based on winkler elastic foundation model," *Building Science*, vol. 31, no. 7, pp. 52–56, 2015.

[18] Y. S. Wang, *Research on Theoretical Analysis Methods for a New Ground Anchor Counterfort Grille–dam*, [Ph.D. Thesis], Lanzhou University of Technology, Lanzhou, China, 2013.

[19] L. R. Xu, Z. Han, Z. M. Su, and Q. Wu, "Research on lateral distribution features of debris flow velocity and structural optimization of prevention and control works," *Rock and Soil Mechanics*, vol. 33, no. 12, pp. 3715–3720, 2010.